

Article

Polymorphism of Bis(benzimidazole)bis(thiocyanato-*N*)cobalt(II) and Its Relevance to Studies of the Chief Color Test for Cocaine

Raychelle Burks ^{1,2} , Francoise M. Amombo Noa ¹  and Lars Öhrström ^{1,*} 

¹ Department of Chemistry and Chemical Engineering, Chalmers University of Technology, 412 96 Gothenburg, Sweden; burks@american.edu (R.B.); mystere@chalmers.se (F.M.A.N.)

² Department of Chemistry, American University, Washington, DC 20016, USA

* Correspondence: ohrstrom@chalmers.se; Tel.: +46-31-772-2871

Abstract: Cobalt(II) thiocyanate-based tests are routinely used to screen cocaine products, with the formation of a blue species interpreted as a positive response. Two popular candidates for the origin of the blue color are an ionic coordination compound, frequently referred to as an ion pair, of the general form $(HL)_2[Co(SCN)_4]$ or the coordination compound $[CoL_2(SCN)_2]$, where L represents select nitrogenous bases. Given the high number of nitrogenous bases documented to yield false positives for cobalt(II) thiocyanate-based tests, a reasonable hypothesis is that both candidates are possible but their preferential formation depends on the specific nitrogenous bases screened. This hypothesis was tested through the crystallographic and spectroscopic analysis of reaction products of cocaine hydrochloride, lidocaine monohydrate hydrochloride, and benzimidazole exposed to a classic cobalt(II) thiocyanate reagent. Single-crystal X-ray diffraction revealed that the blue product isolated from benzimidazole test vessels is a coordination compound, with comparative ultraviolet–visible and Raman spectroscopy validating that blue precipitates collected from cocaine hydrochloride and lidocaine monohydrate hydrochloride reaction containers are ionic coordination compounds. Peaks corresponding to π - π^* transitions in UV-vis at around 320 nm (cocaine hydrochloride: 320 nm, lidocaine hydrochloride: 323 nm) shift to a higher wavelength of 332 nm for the coordinated benzimidazole, and the broader *d-d* transitions at 550–630 nm show both a shift and change in envelope for benzimidazole coordinated with cobalt(II). The compound is a new polymorph of bis(benzimidazole)bis(thiocyanato-*N*)cobalt(II), γ -[Co(Hbzim)₂(SCN)₂] (Hbzim = benzimidazole), and the differences in the intermolecular interactions to the two previous polymorphs were clarified by graph set analysis and Hirshfeld surface analysis. Furthermore, the coordination of aromatic nitrogen bases (such as benzimidazole) with Co(II) and aliphatic bases was compared by analyzing the Cambridge Structural Database, and the aromatic bases were found to have a shorter Co-N bond length compared to the aliphatic bases by around 0.02 Å.

Keywords: cobalt thiocyanate; cocaine; color tests; Raman spectroscopy; ultraviolet–visible (UV–vis) spectroscopy; X-ray diffraction; graph set analysis; Hirshfeld surface analysis



Citation: Burks, R.; Noa, F.M.A.; Öhrström, L. Polymorphism of Bis(benzimidazole)Bis(thiocyanato-*N*)Cobalt(II) and Its Relevance to Studies of the Chief Color Test for Cocaine. *Inorganics* **2024**, *12*, 28. <https://doi.org/10.3390/inorganics12010028>

Academic Editors: Wolfgang Linert, Gabriel García Sánchez, David Turner and Koichiro Takao

Received: 12 December 2023

Revised: 6 January 2024

Accepted: 8 January 2024

Published: 10 January 2024



Copyright: © 2024 by the authors. Licensee MDPI, Basel, Switzerland. This article is an open access article distributed under the terms and conditions of the Creative Commons Attribution (CC BY) license (<https://creativecommons.org/licenses/by/4.0/>).

1. Introduction—Cobalt(II) Thiocyanates

One of the most widespread uses of cobalt(II) thiocyanate is in colorimetric reagents for the forensic screening of suspected cocaine products, with the formation of a blue species implying that such controlled substances are present [1–7]. While these types of color tests are quick and easy to conduct, their chemistry can be complicated, and chromophore identification is an active research area. For the cobalt(II) thiocyanate color tests for cocaine, a long-standing question has been whether cocaine—a nitrogenous base—forms a blue tetra-coordinated entity with the Co(II) ion, or if a blue ionic coordination compound, referred to frequently in the literature and herein as an ion pair, is formed between two

protonated cocaine (cocainium) molecules and a tetrathiocyanatocobaltate anion, such as $(\text{Hcocaine})_2[\text{Co}(\text{SCN})_4]$.

Our recent study probing the product species resulting from reactions between cobalt(II) thiocyanate-based reagents and cocaine hydrochloride, plus the well-documented cocaine product adulterant and color test false-positive lidocaine and its salt, supported that an ion pair is the hallmark blue species formed for these nitrogenous bases [8]. In this work, we expand on our exploration of cobalt(II) thiocyanate-based color tests by studying the blue species produced upon exposure of benzimidazole to a classic cobalt(II) thiocyanate-based reagent (2% *w/v* cobalt(II) thiocyanate in distilled water; hereafter, ‘classic test’). Like cocaine and lidocaine, benzimidazole is a nitrogenous base but with an aromatic amine site, as shown in Figure 1. Cocaine and lidocaine, along with their salts, only contain aliphatic amine sites, a case in point being recent work by Oliver et al. showing that citrate salt of diethylcarbamazine, a nitrogenous base featuring only aliphatic amine sites, yields an ion pair $(\text{Hdiethylcarbamazine})_2[\text{Co}(\text{SCN})_4]$ [9]. Benzimidazole offers an opportunity to explore the impact of aliphatic versus aromatic amine sites on product structure under classic test conditions. We analyzed blue precipitates isolated from cocaine hydrochloride, lidocaine hydrochloride monohydrate, and benzimidazole reaction vessels after screening via the classic test.

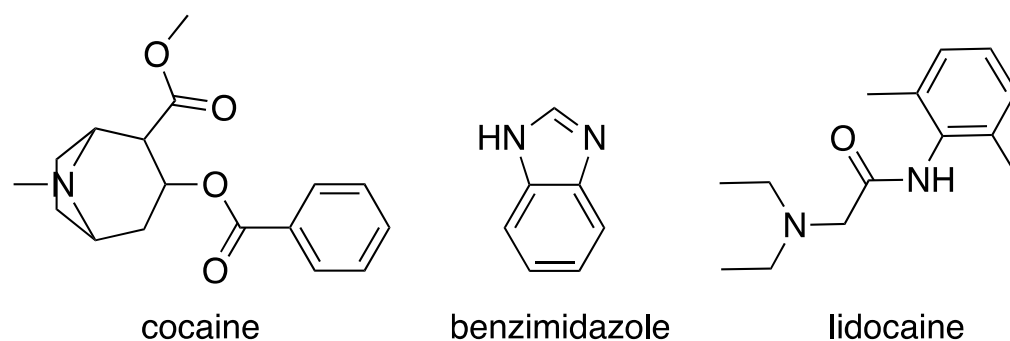


Figure 1. Chemical structures of cocaine, benzimidazole, and lidocaine.

Unlike cocaine, lidocaine, and their salts, the blue species formed upon exposure of benzimidazole to cobalt(II) thiocyanate reagents is the compound $[\text{Co}(\text{Hbzim})_2(\text{SCN})_2]$ (Hbzim = benzimidazole), a neutral coordination entity. There are two different solid-state structures (polymorphs) of $[\text{Co}(\text{Hbzim})_2(\text{SCN})_2]$ in the Cambridge Structural Database (CSD): [10]–GUMXOD [11] and GUMXOD01 [12]. Herein, we report a third polymorph produced upon classic test screening of benzimidazole. The polymorphism displayed by $[\text{Co}(\text{Hbzim})_2(\text{SCN})_2]$ provides valuable insights into the solid-state chemistry of Co(II) tetrahedral complexes in general, but is also relevant for the much studied metal–organic framework ZIF-9, $[\text{Co}(\text{bzim})_2]$, based on tetrahedral Co(II) and benzimidazolate ions [13–15]. The polymorphs GUMXOD α - $[\text{Co}(\text{Hbzim})_2(\text{SCN})_2]$ and GUMXOD01 β - $[\text{Co}(\text{Hbzim})_2(\text{SCN})_2]$ have also been investigated for their magnetic anisotropy and single-ion magnetic properties [11,12]. In this context, the structure and the detailed intermolecular interactions are important, as the metal centers need to be magnetically isolated, thus providing a further reason to compare the structures of the three polymorphs. Note that all polymorphs are N-bonded to Co(II), sometimes indicated as isothiocyanato (for example, in the CSD) or by the IUPAC recommendations as thiocyanato- κN or thiocyanato-N [16].

Critical to cobalt(II) thiocyanate-based color tests, our study highlights the difference in coordination ability between aliphatic and aromatic amines, which is underexplored within the context of cobalt(II) thiocyanate-based color tests. In general, aromatic amines—such as pyridine—are better ligands for transition metals than aliphatic amines [17]. Specifically for tetrahedral Co(II) with two coordinated thiocyanates, there are no non-chelating tertiary amines (such as cocaine) structurally characterized and reported in the CSD. However, in the CSD, there is one chelating tertiary amine, a di-isothiocyanato-

((-)-spartein)-cobalt(II) compound [18], and one secondary amine complex, $[\text{Co}(\text{SCN})_2(1-(2\text{-pyrimidyl})\text{piperazine})_2]$ [19]. Our survey of the CSD also revealed that of the tetrahedral Co(II) compound $[\text{CoA}_2(\text{SCN})_2]$, where A represents aromatic or aliphatic amines, 49 structures feature coordinated aromatic amines, while only two feature aliphatic amines (as mentioned above).

2. Results and Discussion

2.1. Comparison of Blue Products from Classic Test Screening

Single-crystal X-ray diffraction of the blue crystals from the precipitate formed upon screening benzimidazole via the classic test showed that the compound is a new polymorph of $[\text{Co}(\text{Hbzim})_2(\text{SCN})_2]$ designated γ - $[\text{Co}(\text{Hbzim})_2(\text{SCN})_2]$. The molecular structure derived from single-crystal X-ray diffraction determination is shown in Figure 2, and the diffraction data are provided in Table 1.

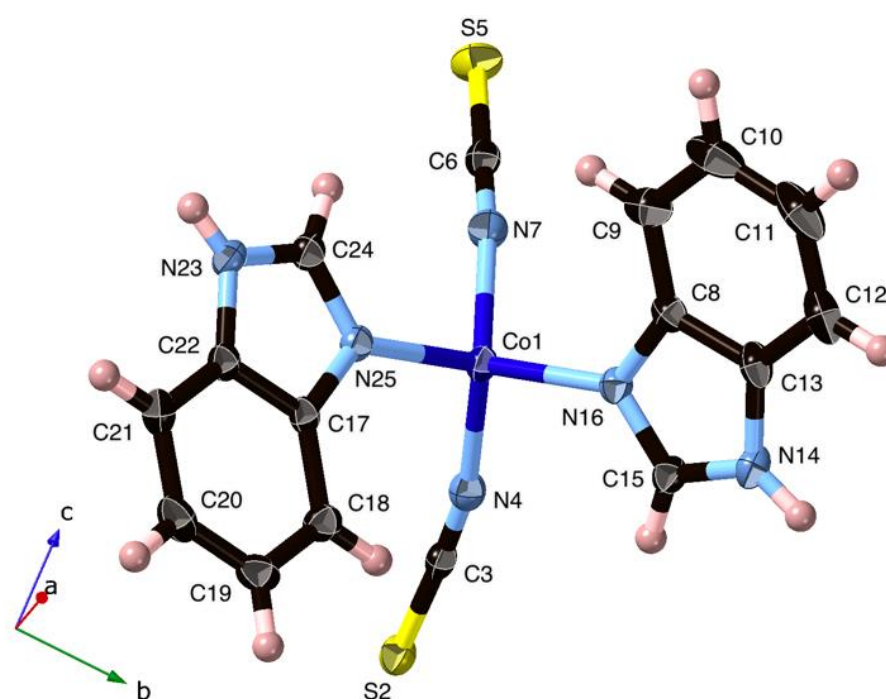


Figure 2. Molecular structure of the new polymorph γ - $[\text{Co}(\text{Hbzim})_2(\text{SCN})_2]$ from single-crystal X-ray diffraction. Displacement ellipsoids drawn at 50%. Note the conformation of the two benzimidazole ligands arranged with benzene rings on opposite sides.

The pertinent bond lengths in $[\text{Co}(\text{Hbzim})_2(\text{SCN})_2]$ are as follows: Co-N_{thiocyanato} Co1-N7 1.949(1) Å and Co1-N4 1.953(1) Å; Co-N_{Hbzim} Co1-N16 1.997(1) Å and Co1-N25 2.002(1) Å; N-C_{thiocyanato} N4-C3 1.161(2) Å and N7-C6 1.161(2) Å; C-S S2-C3 1.632(2) Å and S5-C6 1.619(2) Å. The thiocyanato ligand is near-linear, with angles S2-C3-N4 177.2(1)° and N7-C6-S5 178.8(1)°.

The cobalt(II) ion is in a four-coordinate environment provided by the two benzimidazole and two isothiocyanate ligands, each adopting a monodentate coordination mode. The bond angles at the metal center are as follows: N7-Co1-N16 109.69(6)°; N7-Co1-N25 102.55(6)°; N7-Co1-N4 116.15(6)°; N4-Co1-N16 104.65(6)°; N4-Co1-N25 111.81(6)°, N16-Co1-N25 112.23(5)°. These are all close to the ideal tetrahedral angle, and the angular distortion parameter τ_4 [20] $[(360^\circ - (\alpha + \beta))/141^\circ]$ is 0.93, consistent with a slightly distorted tetrahedral coordination geometry.

Table 1. Selected crystallographic data for γ -[Co(Hbzim)₂(SCN)₂].

Crystal Data	
Chemical formula	C ₁₆ H ₁₂ CoN ₆ S ₂
<i>M_r</i>	411.37
Crystal system, space group	Monoclinic, <i>P</i> 2 ₁ / <i>c</i>
Temperature (K)	125 (2)
<i>a</i> , <i>b</i> , <i>c</i> (Å)	7.83909 (14), 13.5513 (2), 16.7269 (3)
β (°)	96.9887 (17)
<i>V</i> (Å ³)	1763.69 (5)
<i>Z</i>	4
Radiation type	Cu K α
μ (mm ⁻¹)	9.939
Crystal size (mm)	0.066 × 0.065 × 0.052
Data collection	
Diffractometer	XtaLAB Synergy R, HyPix
<i>T</i> _{min} , <i>T</i> _{max}	0.920, 0.967
Index ranges	−7 ≤ <i>h</i> ≤ 9, −16 ≤ <i>k</i> ≤ 16, −20 ≤ <i>l</i> ≤ 20
No. of measured, independent, and observed [<i>I</i> > 2σ(<i>I</i>)] reflections	34139, 3610, 3390
R _{int}	0.040
(sin θ / λ) _{max} (Å ⁻¹)	0.628
Refinement	
<i>R</i> [<i>F</i> ² > 2σ(<i>F</i> ²)], <i>wR</i> (<i>F</i> ²), <i>S</i>	0.0248, 0.0618, 1.044
No. of reflections	3610
No. of parameters	234
$\Delta\rho_{\max}$, $\Delta\rho_{\min}$ (e Å ⁻³)	0.25, −0.20
CCDC nr	2308121

The representative UV–vis spectra of blue species resulting from the classic test screening of lidocaine hydrochloride monohydrate, cocaine hydrochloride and benzimidazole samples dissolved in ethyl acetate are shown in Figure 3. In general, the spectra agree with those presented by Conceição et al. for cocaine, lidocaine, and promethazine, an antihistamine that contains an aliphatic amine site [21]. Peaks around 320 nm (cocaine hydrochloride: 320 nm, lidocaine hydrochloride: 323 nm) have been interpreted as π - π^* transitions of the C \equiv N bond, with a shift to a higher wavelength of 332 nm observed for the coordinated benzimidazole. The broader peaks at 550–630 nm are more complicated, consisting of overlapping bands corresponding to *d-d* transitions [22], with a shift and change in envelope observed for cobalt-bound benzimidazole.

Figure 4 shows the collected Raman spectra of the representative blue precipitate samples from the classic test screening of lidocaine hydrochloride monohydrate, cocaine hydrochloride, and benzimidazole samples, focusing on the characteristic C \equiv N stretching bands around 2100 cm⁻¹, but this stretching frequency alone cannot be used to distinguish between N and S bonded thiocyanato ions [23]. We note that the thiocyanato C–N bond lengths from the structure, 1.161(2) Å, are consistent with a standard C–N triple bond, 1.14 Å [24]. Just as with the UV–vis spectra in Figure 3, we see a clear similarity between the lidocaine hydrochloride monohydrate and cocaine hydrochloride reaction products along with a dissimilarity to γ -[Co(Hbzim)₂(SCN)₂], though such bands appear almost indistinguishable from the noise for the blue benzimidazole screening product. It is well established that the stretching vibrational frequency and/or peak intensity of various nitriles are sensitive to their local hydrogen-bonding and electrostatic environment in addition to temperature [25,26]. However, the low signal-to-noise ratio observed for γ -[Co(Hbzim)₂(SCN)₂] may be due to the sensitivity of the compound to the laser beam.

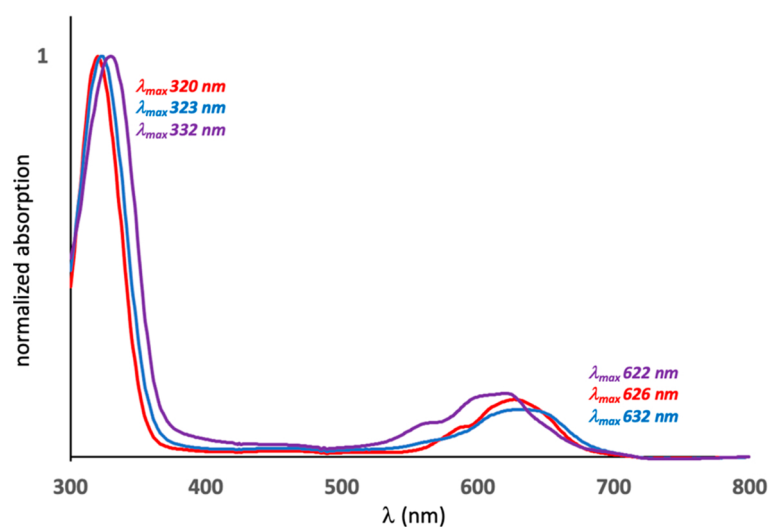


Figure 3. UV-vis spectra in ethyl acetate solution of blue precipitates from cocaine hydrochloride (—), lidocaine monohydrate hydrochloride (—), and benzimidazole (—) reaction products with cobalt thiocyanate.

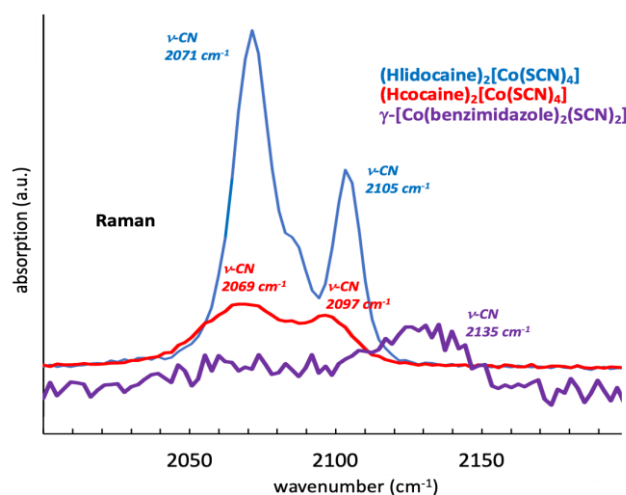


Figure 4. The distinctive Raman bands around 2100 cm^{-1} for blue precipitates retrieved from representative cocaine hydrochloride (—), lidocaine monohydrate hydrochloride (—), and benzimidazole (—) reaction vessels. Usually, these bands are interpreted as $\text{C}\equiv\text{N}$ stretching.

As detailed in our recent work [8], classic test reactions involving lidocaine monohydrate hydrochloride produced blue needle-like crystals $(\text{Hlidocaine})_2([\text{Co}(\text{SCN})_4])\cdot\text{H}_2\text{O}$, while cocaine hydrochloride yielded a glassy, blue material whose amorphous nature made it unsuitable for crystallographic structure determination. However, elemental analysis along with comparative UV-vis, attenuated total reflectance infrared, and Raman spectroscopic analysis strongly supported that the blue material isolated from cocaine hydrochloride reaction vessels was an ion pair $(\text{Hcocaine})_2[\text{Co}(\text{SCN})_4]$. Our work with benzimidazole further showcases the structural similarities between the blue precipitate isolated from cocaine hydrochloride reactions and the structurally characterized ion pair $(\text{Hlidocaine})_2([\text{Co}(\text{SCN})_4])\cdot\text{H}_2\text{O}$ while highlighting how a coordination compound product like $\gamma\text{-}[\text{Co}(\text{Hbzim})_2(\text{SCN})_2]$ differs spectroscopically. These three classic test blue precipitate structures—proposed and confirmed—are shown in Figure 5.

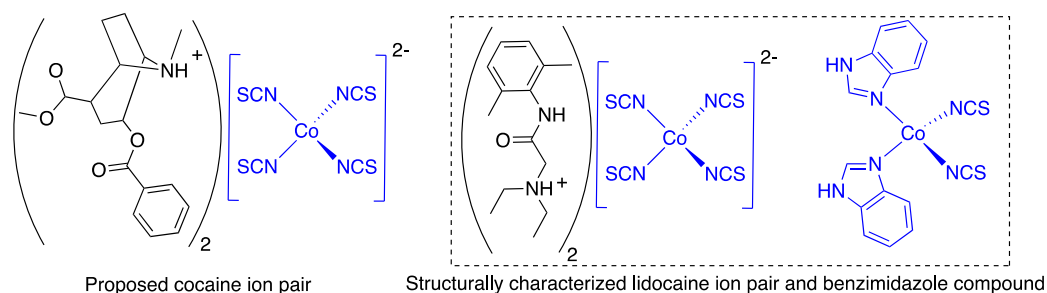


Figure 5. Spectral observations support the formulation of the blue cocaine species as an ion pair (ionic coordination compound) (left) as it shows similarities with the lidocaine ion pair (center) but is different from the benzimidazole coordination compound (right).

It seems that compounds with aromatic amine sites (herein heterocycles) and aliphatic amine sites yield different product types upon reaction with cobalt(II) thiocyanate reagents, and this may be important for the outcome of the test, although in all cases, a blue product is observed. From a purely theoretical point of view, different product types could be expected, as aromatic amines have both occupied π and unoccupied π^* orbitals accessible to interact with the metal center. They are thus potentially both π -acids and π -bases from a coordination chemistry perspective, whereas the aliphatic amines are neither, and the only way they can interact with the metal center is via the free electron pair (thus, as a σ -base) [24]. We further analyzed the CSD to discern trends in aromatic versus aliphatic amine coordination binding strength. To this end, four-coordinated Co(II) structures with at least one coordinated pyridine unit were selected, with pyridine chosen as the archetypal heterocyclic ligand (total number of hits: 614; designated 'Co-N_{pyridinic}') and compared to four-coordinated Co(II) structures with a Co-N bond and a nitrogen with three single bonds to either carbon or hydrogen (total number of hits: 168; designated 'Co-N_{aliphatic}'). Figure 6 shows a comparison of Co-N_{pyridinic} and Co-N_{aliphatic} Co-N bond distances. Although the overlap between the Co-N_{pyridinic} and Co-N_{aliphatic} data sets is large in Figure 6, there is clear preference for a shorter Co-N bond among Co-N_{pyridinic} compounds by about 0.02 Å. It is commonly presumed that a stronger interaction would yield a shorter Co-N bond. The compounds with very short Co-N distances of around 1.8–1.9 Å that can be seen in Figure 6 seem to be mostly related to compounds with so-called pincher ligands with a central pyridine unit.

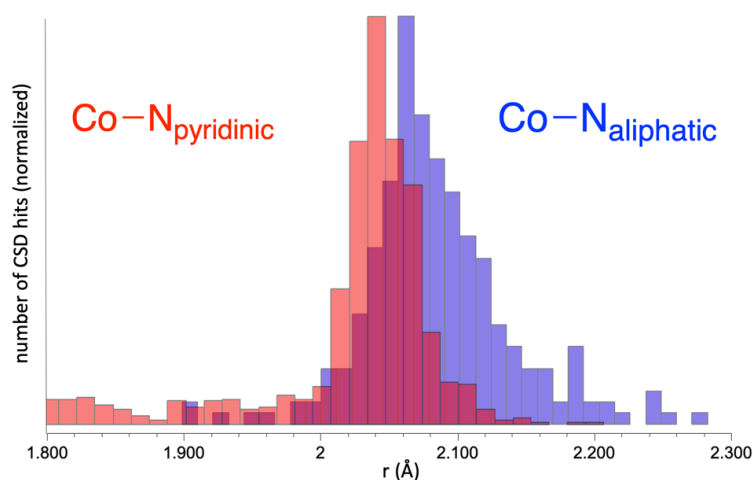


Figure 6. Comparison of four-coordinated Co(II) structures with at least one coordinated pyridine unit (representing aromatic amines; total number of hits: 614) to four-coordinated Co(II) structures with a Co-N bond and a nitrogen with three single bonds to either carbon or hydrogen (total number of hits: 168). The aromatic compounds have a most probable Co-N distance of 2.04 Å and the aliphatic amines a most probable Co-N distance of 2.06 Å.

While the data in Figure 6 support the notion that ion pairs may be more prevalent for aliphatic amines due to their somewhat weaker Co-N bonds, another factor to keep in mind is that aliphatic amines are generally stronger bases than aromatic amines [27]. For example, the pyridinium ion has a pK_a of 5.2, while the triethylammonium ion has a pK_a of 10.8 [27]. We cannot say if it is the greater affinity for metal ions that make complexes more likely for aromatic amines, or if it is their weaker basicity that make ion pairs less likely.

2.2. The Polymorphism of $[\text{Co}(\text{Hbzim})_2(\text{SCN})_2]$

Turning to the polymorphism of $[\text{Co}(\text{Hbzim})_2(\text{SCN})_2]$, we have summarized the differences and similarities in Figures 7 and 8, and Table 2. A few things stand out. First, as illustrated in Figure 8, there are two different conformers: the two benzimidazole ligands are arranged with benzene rings on the same side as in the α -polymorph or on different sides in the β - and γ -polymorph, while the coordination entities of the β - and γ -polymorphs are very close (overlay plots yielding RMSD 0.1232; Max. D: 0.2437; see Figure 7, right). We also see that the two types of Co-N bond lengths (Table 2) are identical within the experimental error and, as expected for the negatively charged thiocyanate groups, the Co-NCS bonds are significantly shorter [28].

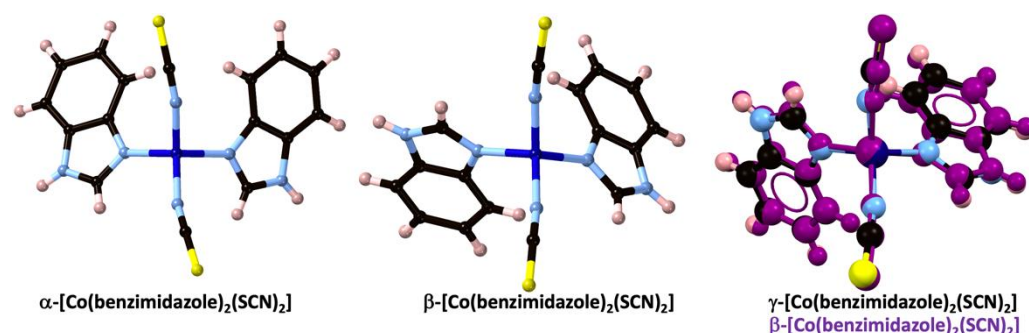


Figure 7. Conformations in the three $[\text{Co}(\text{Hbzim})_2(\text{SCN})_2]$ polymorphs. Note the different conformations of the benzimidazole ligands in α - $[\text{Co}(\text{Hbzim})_2(\text{SCN})_2]$ (left) compared to the β - and γ -polymorphs (center and right) and the close resemblance of the two coordination entities in the β - and γ -polymorphs shown by the overlap plot to the right, as calculated by Mercury.

In principle, coordination (or linkage) isomerism is possible, with a thiocyanate bonding to Co(II) to result in either a Co-NCS or a Co-SCN orientation [29,30] (N- or S-bonding can be indicated, according to the IUPAC recommendations, as thiocyanato- κN , thiocyanato- κS or thiocyanato- N , thiocyanato- S [16], or sometimes also as isothiocyanato for N bonding or thiocyanato for S-bonding, though the latter is ambiguous). However, a search of the CSD may indicate that a Co-SCN isomer is less commonly encountered for cobalt in any oxidation state. For non-bridging thiocyanate ions, we found 1226 Co-NCS hits, but only 15 hits for Co-SCN. Examples of Co-SCN compounds are potassium (ethylenediamine- N,N',N' -triacetato)-thiocyanato-cobalt(III) sesquihydrate [31] (CSD code DIRLOF) and, in bridging mode, thus bonding to both S and N, the yellow coordination polymer $[\text{Co}(\text{SCN})_2(\text{H}_2\text{O})_2]$ [8,32].

The hydrogen bond schemes in the polymorphs can be described using the graph set symbols [33] shown in Table 2 (some can also be seen in Figure 8). The α -polymorph has both 1D chains ($C^1_1(8)$ and $C^4_4(34)$) and rings ($R^2_2(16)$, $R^4_4(32)$, and $R^6_6(48)$). The β -polymorph graph set analysis also shows two 1D chains, and then, two ring hydrogen bonds: $C^1_1(8)$, $C^2_2(16)$, $R^4_4(32)$, and $R^6_6(48)$, respectively. The same types of hydrogen bond graph sets are shown in γ -polymorph $C^1_2(10)$, $C^2_2(16)$, $C^3_4(26)$, and $R^2_2(16)$. Considering this information, it can be concluded that the α -polymorph and β -polymorph are more similar in hydrogen connectivity, with some small differences, as $C^4_4(32)$ and $R^2_2(16)$ are not observed in the β -polymorph. The γ -polymorph is slightly different, with $R^2_2(16)$ seen in the α -polymorph and $C^2_2(16)$ in the β -polymorph. The consequence may be that the α -

and β -polymorphs are less dense, with the γ -polymorph being the most dense and probably the most thermodynamically stable. Finally, the β -polymorph forms hydrogen-bonded sheets in the ab -plane, while the α - and γ -polymorphs form chains along the b -axes.

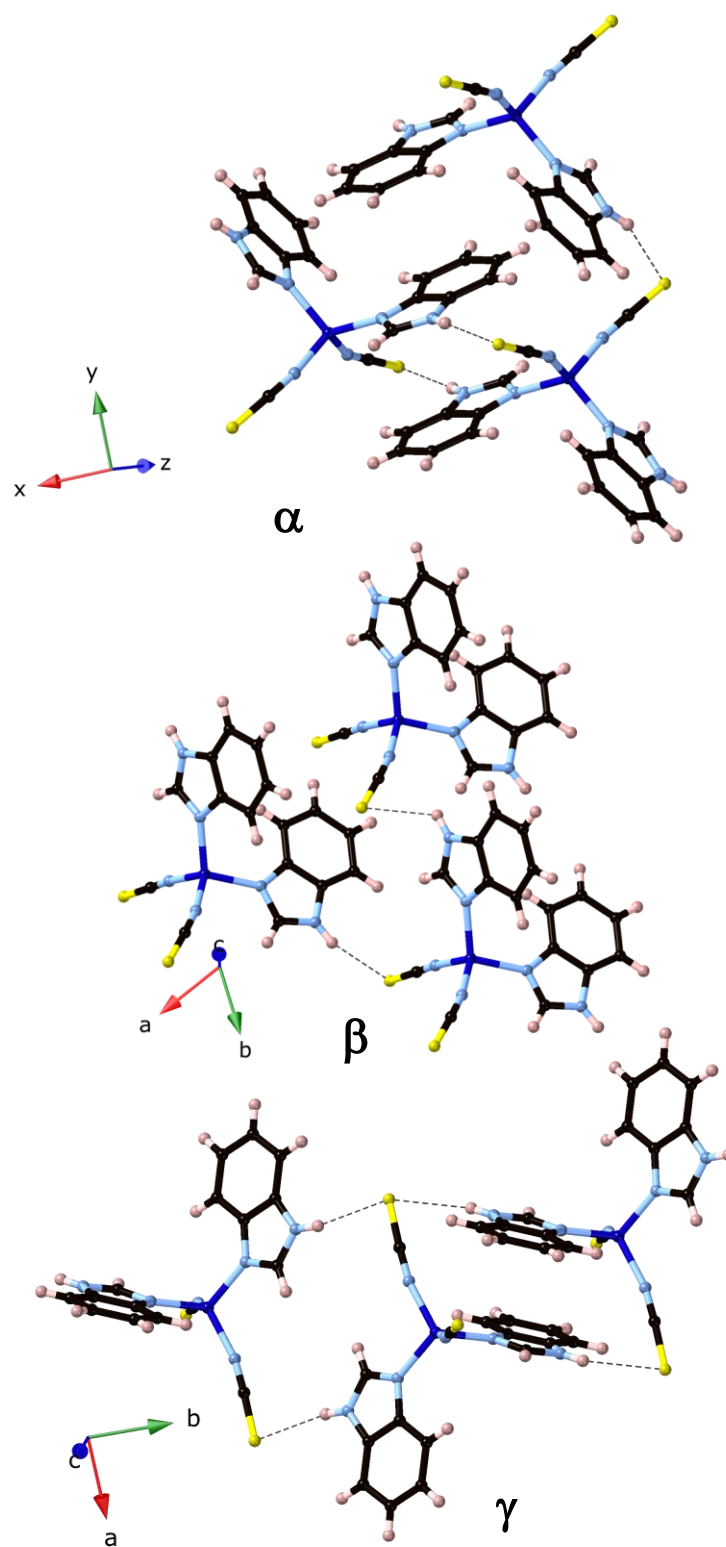
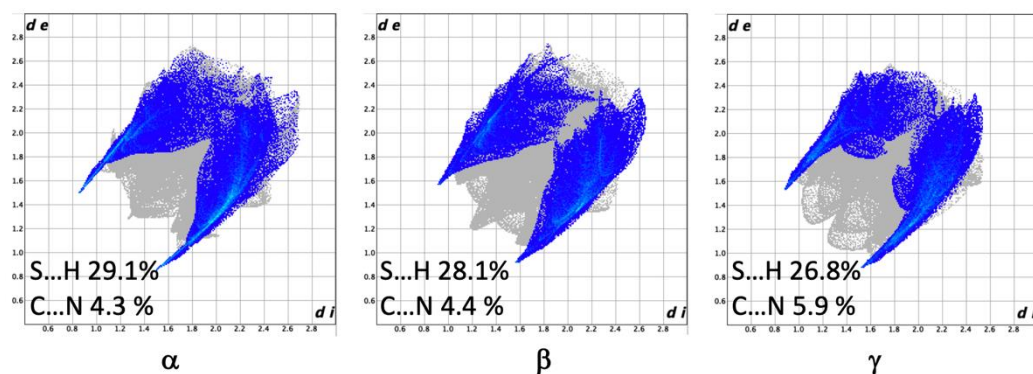


Figure 8. Conformations and hydrogen bonds in the three $[\text{Co}(\text{Hbzim})_2(\text{SCN})_2]$ polymorphs. Some of the graph set symbols in Table 2 can be seen in this figure such as $R^2_2(16)$ for α - $[\text{Co}(\text{Hbzim})_2(\text{SCN})_2]$, $C^1_1(8)$ for β - $[\text{Co}(\text{Hbzim})_2(\text{SCN})_2]$, and $R^2_2(16)$ for γ - $[\text{Co}(\text{Hbzim})_2(\text{SCN})_2]$. Note also the efficient $\pi \cdots \pi$ stacking in the γ -polymorph.

Table 2. Essential characteristics of the three [Co(Hbzim)₂(SCN)₂] polymorphs.

	α [11]	β [12]	γ (This Work)
Space group	$P2_1/n$	$P\bar{1}$	$P2_1/c$
a, b, c (Å)	13.5068(6) 8.3528(4) 16.5567(7)	8.6216(4) 9.3539(4) 12.7307(6)	7.83909(14) 13.5513(2) 16.7269(3)
α, β, γ (°)	90, 104.907(1), 90	75.218(4), 81.213(4), 63.683(4)	90, 96.988(2), 90
T (K)	273	150	125
Density (g/cm ³)	1.518	1.537	1.549
Co-N _{SCN} (Å)	1.951	1.941	1.951
Co-N _{benzimidazole} (Å)	1.998	1.990	2.000
N _{SCN} -Co-N _{SCN} (°)	115.9	115.7	116.1
Hydrogen bonds (Å)	S1-H4 2.515(1) b S2-H2 2.608(2) a	S1-H11 2.60(1) a S2-H12 2.75(1) b	S2-H14 2.54(2) b S2-H23 2.67(2) a
Graph set symbols	R2,2(16) >a> a C1,1(8) b C4,4(32) >a>b<a< b R4,4(32) >a< b >a< b R4,4(32) >a>b<a>b R4,4(32) >a>b>a>b R6,6(48) >a<ba<b<b R6,6(48) >a>b>b<a>b>b R6,6(48) >a>b>b>a>b>b	C1,1(8) a C1,1(8) b C2,2(16) >a<b C2,2(16) >a>b R4,4(32) >a>b<a<b R6,6(48) >a>a>b<a<a< b R6,6(48) >a>b>b<a<b<b	R2,2(16) >a>a R2,2(16) >b>b C1,2(10) >a<b C2,2(16) >a>b C3,4(26) >a>b<a<b

We can further compare the three structures using Hirshfeld surfaces [34]. Hirshfeld surfaces are geometrical representations illustrating intermolecular interactions, such as hydrogen bonding and π - π stacking, and are extensively used in solid-state supramolecular chemistry. As this analysis takes into account all interactions, it is not dependent on the researcher singling out individual measurements to be carried out on the structural data. Also, weaker interactions, including C-H \cdots π , C \cdots H, and H \cdots H contacts, which are sometimes difficult to identify but are still important for crystal packing, can be seen [34]. The most relevant results are shown in Figure 9 as so-called fingerprint plots where individual atom-atom interactions can be selected. Here, we see that there are fewer S...H contacts for the γ -polymorph, while C...N contacts are higher, and we may speculate that this is because of more efficient π \cdots π stacking in the γ -polymorph, as seen in Figure 9 (right).

**Figure 9.** Hirshfeld surface analysis [34], with fingerprint plots. The grey areas show the total interaction plot, and in color, the S...H interactions are highlighted.

3. Materials and Methods

The materials and methods used for this work were first detailed in our recent publication [8] and are also provided here for ease of reference.

3.1. Materials

In-house-produced distilled water was used for all aqueous solutions. All other chemicals were purchased from chemical supply companies such as Sigma-Aldrich (St. Louis, MO, USA) at technical grade or better and were used as received without further purification.

3.2. Single-Crystal X-ray Diffraction

Crystal data, data collection, and structure refinement details are summarized in Table 1. A clear bluish blue block-shaped crystal with dimensions of $0.07 \times 0.07 \times 0.05 \text{ mm}^3$ was mounted on a nylon loop. Data were collected using an XtaLAB Synergy R, HyPix diffractometer operating at $T = 125(2) \text{ K}$ and a wavelength of 1.542 \AA . The diffraction pattern was indexed and the total number of runs and images was based on the strategy calculation from the program *CrysAlis PRO* (Rigaku Europe SE, Neu-Isenburg, Germany, V1.171.42.79a, 2022), and the unit cell was refined using *CrysAlis PRO* (Rigaku, V1.171.42.79a, 2022) on 16,324 reflections. Data reduction, scaling and absorption corrections were performed using *CrysAlis PRO* (Rigaku, V1.171.42.79a, 2022). The final completeness was 100.00% out to 79° in Θ . A Gaussian absorption correction was performed using *CrysAlis PRO* 1.171.42.79a (Rigaku Oxford Diffraction, 2022) based on a Gaussian integration over a multifaceted crystal model, and empirical absorption correction was performed using spherical harmonics, as implemented in the SCALE3 ABSPACK scaling algorithm. The absorption coefficient μ was 9.939 mm^{-1} at this wavelength ($\lambda = 1.542 \text{ \AA}$). The structure was solved and the space group $P2_1/c$ (# 14) determined by the *SHELXT* [35] structure solution program using Intrinsic Phasing and refined via least squares using version 2016/6 of *SHELXL* 2016/6 [35]. All non-hydrogen atoms were refined anisotropically. Hydrogen atom positions were calculated geometrically and refined using the riding model, except for H(N) positions, which were derived from difference maps and refined freely.

3.3. UV-Vis Spectroscopy

For UV-vis analysis, cocaine hydrochloride, lidocaine hydrochloride monohydrate, and benzimidazole samples that provided positive results upon addition of the classic test reagent were used. Ethyl acetate was added directly to selected positive test vials and the resulting blue solution transferred to a new vial and diluted with ethyl acetate. Solutions were passed through $0.45 \text{ }\mu\text{m}$ polytetrafluoroethylene (PTFE) membrane filters prior to UV-vis analysis using a Varian Cary[®] 50 UV-Vis spectrophotometer.

3.4. Raman Spectroscopy

For Raman analysis, a sample was transferred to a glass slide with no additional sample preparation prior to spectra collection. The Raman spectra were collected using an Oxford Instruments alpha300 Raman Imaging Microscope with $10\times$, $50\times$, and $100\times$ objective magnifications. Samples were measured using a 532 nm laser accompanied by grating with 600 grooves/millimeter. To maximize Raman peak clarity and intensity while maintaining precipitate integrity, the laser power, accumulations, and measurement time were varied for each sample analyzed.

3.5. Cobalt(II) Thiocyanate Testing

Classic cobalt(II) thiocyanate test reagent was prepared and administered as detailed in [36]. As noted in the introduction, the classic test reagent was 2% *w/v* cobalt(II) thiocyanate in distilled water. All testing and reagent materials were stored in a temperature-controlled indoor laboratory ($\sim 72^\circ \text{ F}$ or 22° C), being mindful of observed temperature effects on the sensitivity of the cobalt(II) thiocyanate tests [37]. Analyte and reagent amounts

were scaled in tandem for larger experimental yields, as carried out in reference [38]. Samples of cocaine hydrochloride, lidocaine hydrochloride monohydrate, and benzimidazole were subjected to classic test screening. All reaction vessels were evaluated visually, with the assistance of a Zeiss Stemi SV6 microscope, for precipitates that could be evaluated using either single-crystal or powder X-ray diffraction.

3.6. Search of the Cambridge Structural Database (CSD)

The CSD database 5.44 was used as of April 2023. In all runs, Conquest software (version 2023.1.0) was used. For statistical runs, only structures without disorder and with *r* factors of less than 10% were selected. Data were analyzed with Mercury 2023.1.0 (Build 375257).

3.7. Crystallographic Data Treatment

The graph set analysis and overlay plots and calculations were performed using Mercury (Mercury 2023.1.0, Build 375257). Hirshfeld surfaces were calculated using CrystalExplorer (17.5; Revision: f4e298a; Build: 1 May 2017, 11:45). Other structural drawings were created using CrystalMaker (version 10.7.2).

4. Conclusions

In summary, our work further demystifies the differential outcomes of the cobalt(II) thiocyanate-based reagent screening of cocaine products and other nitrogenous bases. While a host of nitrogenous bases yield the hallmark blue positive result to screening, the exact structure of the blue species depends on the presence of aliphatic or aromatic amine sites. For nitrogenous bases with aliphatic amine sites, such as cocaine and lidocaine plus their salts, a positive result is most likely due to the formation of an ion pair (ionic coordination compound) of the general form $(HL)_2[Co(SCN)_4]$. A blue compound of the general form $[CoL_2(SCN)_2]$ is likely the result of the coordination of nitrogenous bases with aromatic amine sites with cobalt(II). The difference noted for the coordinating ability of aliphatic and aromatic amines is significant, as many controlled substances are aliphatic amines, with only a few being aromatic amines [39–41], such as methaqualone [42]. Careful analysis of the CSD data provided additional evidence that the aromatic amines bind more strongly to Co(II) than aliphatic amines, with the most probable Co–N distances shorter by 0.02 Å. The use of graph set symbols unambiguously identified a new polymorph of $[Co(Hbzim)_2(SCN)_2]$ and showed how it differs from the two previously known polymorphs by its different hydrogen bond patterns. Another significant finding was that the α - $[Co(Hbzim)_2(SCN)_2]$ polymorph not only has a different packing and hydrogen bond pattern, but is composed of a different conformer with the benzimidazole ligand rotated 180°. The β - and γ -polymorphs, on the other hand, have very similar coordination entities. This study gives insight into the complexity of these tests, because depending on the conditions of the reactions, a different complex is obtained that has different intermolecular interactions which are essential to understanding the mechanism behind the formation of each blue species.

Author Contributions: Conceptualization, R.B. and L.Ö.; methodology, R.B., F.M.A.N. and L.Ö.; investigation, R.B., F.M.A.N. and L.Ö.; resources, R.B., F.M.A.N. and L.Ö.; writing—original draft preparation, R.B. and L.Ö.; writing—review and editing, R.B., F.M.A.N. and L.Ö.; visualization, L.Ö.; project administration, L.Ö.; funding acquisition, R.B., F.M.A.N. and L.Ö. All authors have read and agreed to the published version of the manuscript.

Funding: Funding for this work was provided by Chalmers University of Technology through the GENIE project and we also thank the Olle Engkvist Foundation for providing funds for the single crystal diffractometer.

Data Availability Statement: Accession Code CCDC 2308121 contains the supplementary crystallographic data for this paper. These data can be obtained free of charge via www.ccdc.cam.ac.uk/data_request/cif, or by emailing data_request@ccdc.cam.ac.uk, or by contacting The Cambridge Crystallographic Data Centre, 12 Union Road, Cambridge CB2 1EZ, UK; Fax: +44-1223-336033. All other data presented in this study are available in the article.

Acknowledgments: This work was carried out in part at the Chalmers Material Analysis Laboratory, CMAL.

Conflicts of Interest: The authors declare no conflicts of interest.

References

1. Nerin, C.; Garnica, A.; Cacho, J. Indirect determination of alkaloids and drugs by atomic absorption spectrometry. *Anal. Chem.* **1985**, *57*, 34–38. [[CrossRef](#)]
2. Schlesinger, H.L. Topics in the chemistry of cocaine. *Bull. Narc.* **1985**, *37*, 63–78.
3. Young, J. The detection of cocaine in the presence of novocaine by means of cobalt thiocyanate. *Am. J. Pharm.* **1931**, *103*, 709–710.
4. Stainier, C. Use of cobalt thiocyanate in the analysis of organic bases. *Il Farm. Ed. Prat.* **1974**, *29*, 119–135.
5. Deltombe, J.; Leboutte, G.; Rosier, N. The application of compounds with a cobalt sulfocyanide base to the determination of alkaloids. *J. Pharm. Belg.* **1962**, *17*, 236–238.
6. Eisman, M.; Gallego, M.; Valcarcel, M. Automatic continuous-flow method for the determination of cocaine. *Anal. Chem.* **1992**, *64*, 1509–1512. [[CrossRef](#)]
7. Shahine, S.; Khamis, S. The spectrophotometric and heterometric determination of some alkaloids as cobalthiocyanates. *Microchem. J.* **1983**, *28*, 26–32. [[CrossRef](#)]
8. Burks, R.; Öhrström, L.; Amombo Noa, F.M. Clarifying the complex chemistry of cobalt(II) thiocyanate-based tests for cocaine using single-crystal X-ray diffraction and spectroscopic techniques. *J. Forensic Sci.* **2024**, *69*, 291–300. [[CrossRef](#)]
9. Oliver, A.G.; Lockwood, T.L.E.; Zinna, J.; Lieberman, M. Bis(N,N-diethyl-4-methyl-4-piperazine-1-carboxamide) tetrakis(isothiocyanato-κN)cobalt(II), a model compound for the blue color developed in the Scott test. *Acta Cryst. E* **2023**, *79*, 163–166. [[CrossRef](#)]
10. Groom, C.R.; Bruno, I.J.; Lightfoot, M.P.; Ward, S.C. The Cambridge Structural Database. *Acta Cryst. B* **2016**, *72*, 171–179. [[CrossRef](#)]
11. Zhang, Z.; Di, D.; Zhai, J.; Wu, L.; Zhu, Q.; Xu, Y.; Huang, R. Synthesis, structures and properties of two complexes based on benzimidazole or benzothiazole ligand. *Chem. Res. Chin. Univ.* **2014**, *30*, 185–189. [[CrossRef](#)]
12. Nemec, I.; Herchel, R.; Trávníček, Z. Suppressing of slow magnetic relaxation in tetracoordinate Co(II) field-induced single-molecule magnet in hybrid material with ferromagnetic barium ferrite. *Sci. Rep.* **2015**, *5*, 10761. [[CrossRef](#)] [[PubMed](#)]
13. Park, K.S.; Ni, Z.; Côté, A.P.; Choi, J.Y.; Huang, R.; Uribe-Romo, F.J.; Chae, H.K.; O’Keeffe, M.; Yaghi, O.M. Exceptional chemical and thermal stability of zeolitic imidazolate frameworks. *Proc. Natl. Acad. Sci. USA* **2006**, *103*, 10186–10191. [[CrossRef](#)] [[PubMed](#)]
14. Zhao, P.; Bennett, T.D.; Casati, N.P.M.; Lampronti, G.I.; Moggach, S.A.; Redfern, S.A.T. Pressure-induced oversaturation and phase transition in zeolitic imidazolate frameworks with remarkable mechanical stability. *Dalton Trans.* **2015**, *44*, 4498–4503. [[CrossRef](#)]
15. Wu, Q.; Zhao, X.L.; Zhou, T.Q.; Jia, A.Z.; Luo, Y.H.; Li, J.D.; Wu, F.C. A metal-organic framework-based electrocatalytic membrane boosts redox kinetics of lithium-sulfur batteries. *J. Energy Storage* **2023**, *72*, 108596. [[CrossRef](#)]
16. Connelly, N.G.; Damhus, T.; Hartshorn, R.M.; Hutton, A.T. *Nomenclature of Inorganic Chemistry IUPAC RECOMMENDATIONS 2005*; International Union of Pure and Applied Chemistry, The Royal Society of Chemistry: Cambridge, UK, 2005.
17. Cotton, F.A.; Wilkinson, G.; Murillo, C.A.; Bochmann, M. *Advanced Inorganic Chemistry*, 6th ed.; Wiley: New York, NY, USA, 1999.
18. Jupp, K.M.; Raithby, P.R. (Dodecahydro-7,14-methano-2H,6H-dipyrido(1,2-a:1',2'-e)(1,5)diazocine-N,N)-di-isothiocyanato-cobalt(ii). *Acta Crystallogr. C* **1992**, *48*, 1214. [[CrossRef](#)]
19. Hannachi, A.; Valkonen, A.; Rzaigui, M.; Smirani, W. Thiocyanate precursor impact on the formation of cobalt complexes: Synthesis and characterization. *Polyhedron* **2019**, *161*, 222–230. [[CrossRef](#)]
20. Yang, L.; Powell, D.R.; Houser, R.P. Structural variation in copper(i) complexes with pyridylmethylamide ligands: Structural analysis with a new four-coordinate geometry index, τ_4 . *Dalton Trans.* **2007**, 955–964. [[CrossRef](#)]
21. Conceição, V.N.; Souza, L.M.; Merlo, B.B.; Filgueiras, P.R.; Poppi, R.J.; Romão, W. Study of scott test using spectroscopic techniques: An alternative method for detecting cocaine hydrochloride and its adulterants in street drugs. *Quim. Nova* **2014**, *37*, 1538–1544. [[CrossRef](#)]
22. Nicholls, D. *The Chemistry of Iron, Cobalt and Nickel*; Pergamon Press: Oxford, UK, 1975; Volume 24, p. 1048.
23. Nakamoto, K. *Infrared Spectra of Inorganic and Coordination Compounds*, 5th ed.; John Wiley & Sons, Inc.: New York, NY, USA, 1997.
24. Atkins, P.; Overton, T.; Rourke, J.; Weller, M.; Armstrong, F. *Shriver & Atkin’s Inorganic Chemistry*; Oxford University Press: Oxford, UK, 2009.
25. Maienschein-Cline, M.G.; Londergan, C.H. The CN stretching band of aliphatic thiocyanate is sensitive to solvent dynamics and specific solvation. *J. Phys. Chem. A* **2007**, *111*, 10020–10025. [[CrossRef](#)]
26. Acharyya, A.; Mukherjee, D.; Gai, F. Assessing the Effect of Hofmeister Anions on the Hydrogen-Bonding Strength of Water via Nitrile Stretching Frequency Shift. *J. Phys. Chem. B* **2020**, *124*, 11783–11792. [[CrossRef](#)]

27. Clayden, J.; Greeves, N.; Warren, S.; Wothers, P. *Organic Chemistry*; Oxford University Press: Oxford, UK, 2000.
28. Nimmermark, A.; Öhrström, L.; Reedijk, J. Metal-ligand bond lengths and strengths: Are they correlated? A detailed CSD analysis. *Z. Kristallogr.* **2013**, *228*, 311–317. [[CrossRef](#)]
29. Burmeister, J.L.; Basolo, F. Inorganic Linkage Isomerism of the Thiocyanate Ion. *Inorg. Chem.* **1964**, *3*, 1587–1593. [[CrossRef](#)]
30. Greenwood, N.N.; Earnshaw, A. *Chemistry of the Elements*, 2nd ed.; Pergamon Press: Oxford, UK, 1997.
31. Yoshikiyo, K.; Hiroaki, I.; Hiroshi, O.; Koshiro, T.; Tasuku, I. Structural Studies of Thiocyanato and Isothiocyanato Cobalt(III) Complexes Ligating Diamine-N,N'-polycarboxylates. *Bull. Chem. Soc. Jpn.* **1985**, *58*, 3506–3512.
32. Cano, F.H.; Garcia-Blanco, S.; Laverat, A.G. The crystal structure of cobalt(II) thiocyanate trihydrate. *Acta Crystallogr. B* **1976**, *32*, 1526–1529. [[CrossRef](#)]
33. Etter, M.C.; MacDonald, J.C.; Bernstein, J. Graph-set analysis of hydrogen-bond patterns in organic crystals. *Acta Crystallogr. B* **1990**, *46*, 256–262. [[CrossRef](#)]
34. Spackman, M.A.; Jayatilaka, D. Hirshfeld surface analysis. *Crystengcomm* **2009**, *11*, 19–32. [[CrossRef](#)]
35. Sheldrick, G.M. Crystal structure refinement with SHELXL. *Acta Crystallogr. C* **2015**, *71*, 3–8. [[CrossRef](#)]
36. *NIJ standard-0604.01*; Color Test Reagents/Kits for Pre-Liminary Identification of Drugs of Abuse. Department of Justice, National Institute of Justice: Washington, DC, USA, 2000.
37. McGill, J.W.; Dixon, C.; Ritter, D.; Girardeau, C.; Sides, J.D. Discovery of an Interesting Temperature Effect on the Sensitivity of the Cobalt Thiocyanate Test for Cocaine. *Microgram* **2008**, *6*, 26–35.
38. de Souza, D.M.; de Moura Messias, P.J.; Silva Santos, I.d.; Ramalho, E.D.; Ferrari Júnior, E.; de Oliveira Morais, P.A. Scott test associated with multivariate image analysis: A more selective alternative for cocaine research in forensic laboratories. *Forensic Sci. Int.* **2022**, *335*, 111277. [[CrossRef](#)]
39. Appendino, G.; Minassi, A.; Tagliatalata-Scafati, O. Recreational drug discovery: Natural products as lead structures for the synthesis of smart drugs. *Nat. Prod. Rep.* **2014**, *31*, 880–904. [[CrossRef](#)] [[PubMed](#)]
40. Hondebrink, L.; Zwartsen, A.; Westerink, R.H.S. Effect fingerprinting of new psychoactive substances (NPS): What can we learn from in vitro data? *Pharmacol. Ther.* **2018**, *182*, 193–224. [[CrossRef](#)] [[PubMed](#)]
41. United Nations. *The International Drug Control Conventions, Schedules of the Single Convention on Narcotic Drugs of 1961 as Amended by the 1972 Protocol, as at 18 May 2016*; United Nations: New York, NY, USA, 2016.
42. Alliston, G.V.; Bartlett, A.F.F.; de Faubert Maunder, M.J.; Phillips, G.F. An improved test for cocaine, methaqualone and methadone with a modified cobalt(II) thiocyanate reagent. *Analyst* **1972**, *97*, 263–265. [[CrossRef](#)] [[PubMed](#)]

Disclaimer/Publisher's Note: The statements, opinions and data contained in all publications are solely those of the individual author(s) and contributor(s) and not of MDPI and/or the editor(s). MDPI and/or the editor(s) disclaim responsibility for any injury to people or property resulting from any ideas, methods, instructions or products referred to in the content.